Fermilab FERMILAB-Pub-01/063-E CDF May 2001

Double Diffraction Dissociation at the Fermilab Tevatron Collider

T. Affolder,[23] H. Akimoto,[45] A. Akopian,[37] M. G. Albrow,[11] P. Amaral,[8] D. Amidei,[25] K. Anikeev,[24] J. Antos,[1] G. Apollinari,[11] T. Arisawa,[45] T. Asakawa,[43] W. Ashmanskas,[8] F. Azfar,[30] P. Azzi-Bacchetta,[31] N. Bacchetta,[31] M. W. Bailey,[27] S. Bailey,[16] P. de Barbaro,[36] A. Barbaro-Galtieri,[23] V. E. Barnes,[35] B. A. Barnett,[19] S. Baroiant,[5] M. Barone,[13] G. Bauer,[24] F. Bedeschi,[33] S. Belforte,[42] W. H. Bell,[15] G. Bellettini,[33] J. Bellinger,[46] D. Benjamin,[10] J. Bensinger,[4] A. Beretvas,[11] J. P. Berge,[11] J. Berryhill,[8] A. Bhatti,[37] M. Binkley,[11] D. Bisello,[31] M. Bishai,[11] R. E. Blair,[2] C. Blocker,[4] K. Bloom,[25] B. Blumenfeld,[19] S. R. Blusk,[36] A. Bocci,[37] A. Bodek,[36] W. Bokhari,[32] G. Bolla,[35] Y. Bonushkin,[6] D. Bortoletto,[35] J. Boudreau,[34] A. Brandl,[27] S. van den Brink,[19] C. Bromberg,[26] M. Brozovic,[10] N. Bruner,[27] E. Buckley-Geer,[11] J. Budagov,[9] H. S. Budd,[36] K. Burkett,[16] G. Busetto,[31] A. Byon-Wagner,[11] K. L. Byrum,[2] S. Cabrera,[10] P. Calafiura,[23] M. Campbell,[25] W. Carithers,[23] J. Carlson,[25] D. Carlsmith,[46] W. Caskey,[5] A. Castro,[3] D. Cauz,[42] A. Cerri,[33] A. W. Chan,[1] P. S. Chang,[1] P. T. Chang,[1] J. Chapman,[25] C. Chen,[32] Y. C. Chen,[1] M. -T. Cheng,[1] M. Chertok,[5] G. Chiarelli,[33] I. Chirikov-Zorin,[9] G. Chlachidze,[9] F. Chlebana,[11] L. Christofek,[18] M. L. Chu,[1] Y. S. Chung,[36] C. I. Ciobanu,[28] A. G. Clark,[14] A. Connolly,[23] M. Convery,[37] J. Conway,[38] M. Cordelli,[13] J. Cranshaw,[40] R. Cropp,[41] R. Culbertson,[11] D. Dagenhart,[44] S. D'Auria,[15] F. DeJongh,[11] S. Dell'Agnello,[13] M. Dell'Orso,[33] L. Demortier,[37] M. Deninno,[3] P. F. Derwent,[11] T. Devlin,[38] J. R. Dittmann,[11] A. Dominguez,[23] S. Donati,[33] J. Done,[39] M. D'Onofrio,[33] T. Dorigo,[16] N. Eddy,[18] K. Einsweiler,[23] J. E. Elias,[11] E. Engels, Jr.,[34] R. Erbacher,[11] D. Errede,[18] S. Errede,[18] Q. Fan,[36] R. G. Feild,[47] J. P. Fernandez,[11] C. Ferretti,[33] R. D. Field,[12] I. Fiori,[3] B. Flaugher,[11] G. W. Foster,[11] M. Franklin,[16] J. Freeman,[11] J. Friedman,[24] Y. Fukui,[22] I. Furic,[24] S. Galeotti,[33] A. Gallas,[(**) 16] M. Gallinaro,[37] T. Gao,[32] M. Garcia-Sciveres,[23] A. F. Garfinkel,[35] P. Gatti,[31] C. Gay,[47] D. W. Gerdes,[25] P. Giannetti,[33] V. Glagolev,[9] D. Glenzinski,[11] M. Gold,[27] J. Goldstein,[11] I. Gorelov,[27] A. T. Goshaw,[10]

Y. Gotra,[34] K. Goulianos,[37] C. Green,[35] G. Grim,[5] P. Gris,[11] L. Groer,[38] C. Grosso-Pilcher,[8] M. Guenther,[35] G. Guillian,[25] J. Guimaraes da Costa,[16] R. M. Haas,[12] C. Haber,[23] S. R. Hahn,[11] C. Hall,[16] T. Handa,[17] R. Handler,[46] W. Hao,[40] F. Happacher,[13] K. Hara,[43] A. D. Hardman,[35] R. M. Harris,[11] F. Hartmann,[20] K. Hatakeyama,[37] J. Hauser,[6] J. Heinrich,[32] A. Heiss,[20] M. Herndon,[19] C. Hill,[5] K. D. Hoffman,[35] C. Holck,[32] R. Hollebeek,[32] L. Holloway,[18] R. Hughes,[28] J. Huston,[26] J. Huth,[16] H. Ikeda,[43] J. Incandela,[11] G. Introzzi,[33] J. Iwai,[45] Y. Iwata,[17] E. James,[25] M. Jones,[32] U. Joshi,[11] H. Kambara,[14] T. Kamon,[39] T. Kaneko,[43] K. Karr,[44] H. Kasha,[47] Y. Kato,[29] T. A. Keaffaber,[35] K. Kelley,[24] M. Kelly,[25] R. D. Kennedy,[11] R. Kephart,[11] D. Khazins,[10] T. Kikuchi,[43] B. Kilminster,[36] B. J. Kim,[21] D. H. Kim,[21] H. S. Kim,[18] M. J. Kim,[21] S. B. Kim,[21] S. H. Kim,[43] Y. K. Kim,[23] M. Kirby,[10] M. Kirk,[4] L. Kirsch,[4] S. Klimenko,[12] P. Koehn,[28] K. Kondo,[45] J. Konigsberg,[12] A. Korn,[24] A. Korytov,[12] E. Kovacs,[2] J. Kroll,[32] M. Kruse,[10] S. E. Kuhlmann,[2] K. Kurino,[17] T. Kuwabara,[43] A. T. Laasanen,[35] N. Lai,[8] S. Lami,[37] S. Lammel,[11] J. Lancaster,[10] M. Lancaster,[23] R. Lander,[5] G. Latino,[33] T. LeCompte,[2] A. M. Lee IV,[10] K. Lee,[40] S. Leone,[33] J. D. Lewis,[11] M. Lindgren,[6] T. M. Liss,[18] J. B. Liu,[36] Y. C. Liu,[1] D. O. Litvintsev,[11] O. Lobban,[40] N. Lockyer,[32] J. Loken,[30] M. Loreti,[31] D. Lucchesi,[31] P. Lukens,[11] S. Lusin,[46] L. Lyons,[30] J. Lys,[23] R. Madrak,[16] K. Maeshima,[11] P. Maksimovic,[16] L. Malferrari,[3] M. Mangano,[33] M. Mariotti,[31] G. Martignon,[31] A. Martin,[47] J. A. J. Matthews,[27] J. Mayer,[41] P. Mazzanti,[3] K. S. McFarland,[36] P. McIntyre,[39] E. McKigney,[32] M. Menguzzato,[31] A. Menzione,[33] C. Mesropian,[37] A. Meyer,[11] T. Miao,[11] R. Miller,[26] J. S. Miller,[25] H. Minato,[43] S. Miscetti,[13] M. Mishina,[22] G. Mitselmakher,[12] N. Moggi,[3] E. Moore,[27] R. Moore,[25] Y. Morita,[22] T. Moulik,[35] M. Mulhearn,[24] A. Mukherjee,[11] T. Muller,[20] A. Munar,[33] P. Murat,[11] S. Murgia,[26] J. Nachtman,[6] V. Nagaslaev,[40] S. Nahn,[47] H. Nakada,[43] I. Nakano,[17] C. Nelson,[11] T. Nelson,[11] C. Neu,[28] D. Neuberger,[20] C. Newman-Holmes,[11] C.-Y. P. Ngan,[24] H. Niu,[4] L. Nodulman,[2] A. Nomerotski,[12] S. H. Oh,[10] Y. D. Oh,[21] T. Ohmoto,[17] T. Ohsugi,[17] R. Oishi,[43] T. Okusawa,[29] J. Olsen,[46] W. Orejudos,[23] C. Pagliarone,[33] F. Palmonari,[33] R. Paoletti,[33] V. Papadimitriou,[40] D. Partos,[4] J. Patrick,[11] G. Pauletta,[42] M. Paulini,[(*) 23] C. Paus,[24] L. Pescara,[31] T. J. Phillips,[10] G. Piacentino,[33] K. T. Pitts,[18]

A. Pompos,[35] L. Pondrom,[46] G. Pope,[34] M. Popovic,[41] F. Prokoshin,[9] J. Proudfoot,[2] F. Ptohos,[13] O. Pukhov,[9] G. Punzi,[33] A. Rakitine,[24] D. Reher,[23] A. Reichold,[30] A. Ribon,[31] W. Riegler,[16] F. Rimondi,[3] L. Ristori,[33] M. Riveline,[41] W. J. Robertson,[10] A. Robinson,[41] T. Rodrigo,[7] S. Rolli,[44] L. Rosenson,[24] R. Roser,[11] R. Rossin,[31] A. Roy,[35] A. Ruiz,[7] A. Safonov,[12] R. St. Denis,[15] W. K. Sakumoto,[36] D. Saltzberg,[6] C. Sanchez,[28] A. Sansoni,[13] L. Santi,[42] H. Sato,[43] P. Savard,[41] P. Schlabach,[11] E. E. Schmidt,[11] M. P. Schmidt,[47] M. Schmitt,[(**) 16] L. Scodellaro,[31] A. Scott,[6] A. Scribano,[33] S. Segler,[11] S. Seidel,[27] Y. Seiya,[43] A. Semenov,[9] F. Semeria,[3] T. Shah,[24] M. D. Shapiro,[23] P. F. Shepard,[34] T. Shibayama,[43] M. Shimojima,[43] M. Shochet,[8] A. Sidoti,[31] J. Siegrist,[23] A. Sill,[40] P. Sinervo,[41] P. Singh,[18] A. J. Slaughter,[47] K. Sliwa,[44] C. Smith,[19] F. D. Snider,[11] A. Solodsky,[37] J. Spalding,[11] T. Speer,[14] P. Sphicas,[24] F. Spinella,[33] M. Spiropulu,[16] L. Spiegel,[11] J. Steele,[46] A. Stefanini,[33] J. Strologas,[18] F. Strumia, [14] D. Stuart,[11] K. Sumorok,[24] T. Suzuki,[43] T. Takano,[29] R. Takashima,[17] K. Takikawa,[43] P. Tamburello,[10] M. Tanaka,[43] B. Tannenbaum,[6] M. Tecchio,[25] R. Tesarek,[11] P. K. Teng,[1] K. Terashi,[37] S. Tether,[24] A. S. Thompson,[15] R. Thurman-Keup,[2] P. Tipton,[36] S. Tkaczyk,[11] D. Toback,[39] K. Tollefson,[36] A. Tollestrup,[11] D. Tonelli,[33] H. Toyoda,[29] W. Trischuk,[41] J. F. de Troconiz,[16] J. Tseng,[24] N. Turini,[33] F. Ukegawa,[43] T. Vaiciulis,[36] J. Valls,[38] S. Vejcik III,[11] G. Velev,[11] R. Vidal,[11] I. Vila,[7] R. Vilar,[7] I. Volobouev,[23] D. Vucinic,[24] R. G. Wagner,[2] R. L. Wagner,[11] N. B. Wallace,[38] C. Wang,[10] M. J. Wang,[1] B. Ward,[15] S. Waschke,[15] T. Watanabe,[43] D. Waters,[30] T. Watts,[38] R. Webb,[39] H. Wenzel,[20] W. C. Wester III,[11] A. B. Wicklund,[2] E. Wicklund,[11] T. Wilkes,[5] H. H. Williams,[32] P. Wilson,[11] B. L. Winer,[28] D. Winn,[25] S. Wolbers,[11] D. Wolinski,[25] J. Wolinski,[26] S. Wolinski,[25] S. Worm,[27] X. Wu,[14] J. Wyss,[33] A. Yagil,[11] W. Yao,[23] G. P. Yeh,[11] P. Yeh,[1] J. Yoh,[11] C. Yosef,[26] T. Yoshida,[29] I. Yu,[21] S. Yu,[32] Z. Yu,[47] A. Zanetti,[42] F. Zetti,[23] and S. Zucchelli[3]

(CDF Collaboration)

[1] *Institute of Physics, Academia Sinica, Taipei, Taiwan 11529, Republic of China*

[2] *Argonne National Laboratory, Argonne, Illinois 60439*

[3] *Istituto Nazionale di Fisica Nucleare, University of Bologna, I-40127 Bologna, Italy*

[4] *Brandeis University, Waltham, Massachusetts 02254*

[5] *University of California at Davis, Davis, California 95616*

[6] *University of California at Los Angeles, Los Angeles, California 90024*

[7] *Instituto de Fisica de Cantabria, CSIC-University of Cantabria, 39005 Santander, Spain*

[8] *Enrico Fermi Institute, University of Chicago, Chicago, Illinois 60637*

[9] *Joint Institute for Nuclear Research, RU-141980 Dubna, Russia*

[10] *Duke University, Durham, North Carolina 27708*

[11] *Fermi National Accelerator Laboratory, Batavia, Illinois 60510*

[12] *University of Florida, Gainesville, Florida 32611*

[13] *Laboratori Nazionali di Frascati, Istituto Nazionale di Fisica Nucleare, I-00044 Frascati, Italy*

[14] *University of Geneva, CH-1211 Geneva 4, Switzerland*

[15] *Glasgow University, Glasgow G12 8QQ, United Kingdom*

[16] *Harvard University, Cambridge, Massachusetts 02138*

[17] *Hiroshima University, Higashi-Hiroshima 724, Japan*

[18] *University of Illinois, Urbana, Illinois 61801*

[19] *The Johns Hopkins University, Baltimore, Maryland 21218*

[20] *Institut für Experimentelle Kernphysik, Universität Karlsruhe, 76128 Karlsruhe, Germany*

[21] *Center for High Energy Physics: Kyungpook National University, Taegu 702-701; Seoul National University, Seoul 151-742; and SungKyunKwan University, Suwon 440-746; Korea*

[22] *High Energy Accelerator Research Organization (KEK), Tsukuba, Ibaraki 305, Japan*

[23] *Ernest Orlando Lawrence Berkeley National Laboratory, Berkeley, California 94720*

[24] *Massachusetts Institute of Technology, Cambridge, Massachusetts 02139*

[25] *University of Michigan, Ann Arbor, Michigan 48109*

[26] *Michigan State University, East Lansing, Michigan 48824*

[27] *University of New Mexico, Albuquerque, New Mexico 87131*

[28] *The Ohio State University, Columbus, Ohio 43210*

[29] Osaka City University, Osaka 588, Japan

[30] University of Oxford, Oxford OX1 3RH, United Kingdom

[31] Universita di Padova, Istituto Nazionale di Fisica Nucleare, Sezione di Padova, I-35131 Padova, Italy

[32] University of Pennsylvania, Philadelphia, Pennsylvania 19104

[33] Istituto Nazionale di Fisica Nucleare, University and Scuola Normale Superiore of Pisa, I-56100 Pisa, Italy

[34] University of Pittsburgh, Pittsburgh, Pennsylvania 15260

[35] Purdue University, West Lafayette, Indiana 47907

[36] University of Rochester, Rochester, New York 14627

[37] Rockefeller University, New York, New York 10021

[38] Rutgers University, Piscataway, New Jersey 08855

[39] Texas A&M University, College Station, Texas 77843

[40] Texas Tech University, Lubbock, Texas 79409

[41] Institute of Particle Physics, University of Toronto, Toronto M5S 1A7, Canada

[42] Istituto Nazionale di Fisica Nucleare, University of Trieste/ Udine, Italy

[43] University of Tsukuba, Tsukuba, Ibaraki 305, Japan

[44] Tufts University, Medford, Massachusetts 02155

[45] Waseda University, Tokyo 169, Japan

[46] University of Wisconsin, Madison, Wisconsin 53706

[47] Yale University, New Haven, Connecticut 06520

(*) Now at Carnegie Mellon University, Pittsburgh, Pennsylvania 15213

(**) Now at Northwestern University, Evanston, Illinois 60208

Abstract

We present results from a measurement of double diffraction dissociation in $\bar{p}p$ collisions at the Fermilab Tevatron collider. The production cross section for events with a central pseudorapidity gap of width $\Delta\eta^0 > 3$

(overlapping $\eta = 0$) is found to be 4.43 ± 0.02(stat)± 1.18(syst) mb [3.42 ± 0.01(stat)± 1.09(syst) mb] at $\sqrt{s} = 1800$ [630] GeV. Our results are compared with previous measurements and with predictions based on Regge theory and factorization.

PACS number(s): 13.85.Ni

Double diffraction (DD) dissociation is the process in which two colliding hadrons dissociate into clusters of particles producing events with a central pseudorapidity [1] gap (region of pseudorapidity devoid of particles), as shown in Fig. 1. This process is similar to single diffraction (SD) dissociation, in which one of the incident hadrons dissociates while the other escapes as a leading (highest momentum) particle. Events with pseudorapidity gaps are presumed to be due to the exchange across the gap of a Pomeron [2], which in QCD is a color singlet state with vacuum quantum numbers.

Previous measurements of DD have been performed only over limited pseudorapidity regions for $\bar{p}p$ collisions at $\sqrt{s}$ = 200 and 900 GeV [3], for exclusive and semi-inclusive dissociation channels at lower energies [4,5], e.g $pp \to (p\pi^+\pi^-)(p\pi^+\pi^-)$ or $pp \to (p\pi^+\pi^-) + X$, and for γp interactions at the DESY ep collider HERA [6]. The present measurement, based on a study of central rapidity gaps in minimum bias events from $\bar{p}p$ collisions at $\sqrt{s}$ = 1800 and 630 GeV collected by the Collider Detector at Fermilab (CDF), covers a wide η range, allowing comparisons with theoretical predictions on both η-dependence and normalization.

To facilitate our discussion, we begin by defining the relevant variables [7]. We use s and t for the square of the c.m.s. energy and 4-momentum transfer between the two incident hadrons, ξ for the fractional momentum loss of the leading hadron in SD, and η for pseudorapidity. For $\bar{p}p$ double diffraction dissociation into masses M_1 and M_2, we define the *nominal* pseudorapidity gap as $\Delta\eta \equiv \ln \frac{ss_\circ}{M_1^2 M_2^2}$, where $s_\circ \equiv 1$ GeV^2; on average, the nominal gap is approximately equal to the true rapidity gap in an event. A variable defined as $s' \equiv M_1^2 M_2^2/s_\circ$ can be thought of as the s-value of the diffractive sub-system since $\ln \frac{s'}{s_\circ}$ represents the pseudorapidity region accessible to the dissociation products of M_1 and M_2; for $\bar{p}p$ SD with $M_2 = m_p \approx 1$ GeV, $s' = M_1^2$ and $\xi = e^{-\Delta\eta} = s'/s$.

Diffraction has traditionally been treated theoretically in the framework of Regge phenomenology [2]. At large $\Delta\eta$, where Pomeron exchange is dominant [7], the SD cross section is given by the triple-Pomeron amplitude,

$$\frac{d^2\sigma_{SD}}{dtd\Delta\eta} = \left[\frac{\beta^2(t)}{16\pi}e^{2[\alpha(t)-1]\Delta\eta}\right]\left[\kappa\beta^2(0)\left(\frac{s'}{s_\circ}\right)^{\alpha(0)-1}\right] \tag{1}$$

where $\alpha(t)$ is the Pomeron trajectory, $\beta(t)$ the coupling of the Pomeron to the (anti)proton, and $\kappa \equiv g(t)/\beta(0)$ the ratio of the triple-Pomeron to the Pomeron-proton couplings; we use $\alpha(t) = \alpha(0) + \alpha' t = 1.104 + 0.25t$ [8], $\beta(0) = 4.1$ mb$^{1/2}$ [8], and $g(t) = 0.69$ mb$^{1/2}$ ($\Rightarrow \kappa = 0.17$) [9]. The second factor of Eq. 1 has the form of the Pomeron-proton total cross section at the sub-energy $\sqrt{s'}$, while the first factor can be thought of as a rapidity gap probability [10]. Measurements on SD have shown that Eq. 1, which is based on Regge factorization, correctly predicts the $\Delta\eta$ dependence for $\Delta\eta > 3$, but fails to predict the energy dependence of the overall normalization, which at $\sqrt{s} = 1800$ GeV is found to be suppressed by an order of magnitude [11,12]. It is generally believed that this breakdown of factorization is imposed by unitarity constraints [13]. Phenomenologically, it has been shown that normalizing the integral of the gap probability (first factor in Eq. 1) over all phase space to unity yields the correct energy dependence [9,12].

Using factorization, the DD differential cross section may be expressed in terms of the SD and elastic scattering cross sections as [7]

$$\begin{aligned}\frac{d^3\sigma_{DD}}{dtdM_1^2dM_2^2} &= \frac{d^2\sigma_{SD}}{dtdM_1^2}\frac{d^2\sigma_{SD}}{dtdM_2^2} \Big/ \frac{d\sigma_{el}}{dt} \\ &= \frac{[\kappa\beta_1(0)\beta_2(0)]^2}{16\pi}\,\frac{s^{2[\alpha(0)-1]}\,e^{b_{DD}t}}{(M_1^2M_2^2)^{1+2[\alpha(0)-1]}}\end{aligned} \tag{2}$$

where $b_{DD} = 2\alpha' \ln(ss_\circ/M_1^2M_2^2)$. Changing variables from M_1 and M_2 to $\Delta\eta$ and $\eta_c = \ln\frac{M_2}{M_1}$, where η_c is the center of the rapidity gap, yields (setting $\beta_1 = \beta_2 \Rightarrow \beta$)

$$\frac{d^3\sigma_{DD}}{dtd\Delta\eta d\eta_c} = \left[\frac{\kappa\beta^2(0)}{16\pi}e^{2[\alpha(t)-1]\Delta\eta}\right]\left[\kappa\beta^2(0)\left(\frac{s'}{s_\circ}\right)^{\alpha(0)-1}\right] \tag{3}$$

This expression is strikingly similar to Eq. 1, except that, since the gap is now not adjacent to a leading (anti)proton, η_c is treated as an independent variable. The question that arises naturally is whether Eq. 3 correctly predicts the differential DD cross section apart from an overall normalization factor, as is the case with Eq. 1 for SD. The answer to this question, and the suppression in overall normalization relative to that observed in SD, could provide a crucial check on models proposed to account for the factorization breakdown observed in SD.

The components of CDF [14] relevant to this study are the central tracking chamber (CTC), the calorimeters, and two scintillation beam-beam counter (BBC) arrays. The CTC tracking efficiency varies from $\sim 60\%$ for $p_T = 300$ MeV to over 95% for $p_T > 400$ MeV within $|\eta| < 1.2$, and falls monotonically beyond $|\eta| = 1.2$ approaching zero at $|\eta| \sim 1.8$. The calorimeters have projective tower geometry and cover the regions $|\eta| < 1.1$ (central), $1.1 < |\eta| < 2.4$ (plug), and $2.2 < |\eta| < 4.2$ (forward). The $\Delta\eta \times \Delta\phi$ tower dimensions are $0.1 \times 15^\circ$ for the central and $0.1 \times 5^\circ$ for the plug and forward calorimeters. The BBC arrays cover the region $3.2 < |\eta| < 5.9$.

Events collected by triggering on a BBC coincidence between the proton and antiproton sides of the detector comprise the CDF *minimum-bias* (MB) data sample. Two MB data sets are used in this analysis, consisting of 1.0×10^6 (1.6×10^6) events at $\sqrt{s} = 1800$ [630] GeV obtained at average instantaneous luminosities of 2.5×10^{30} (9.6×10^{29}) cm^{-2}sec^{-1}. At these luminosities, the fraction of *overlap* events due to multiple interactions is estimated to be 20.7 (6.5)%. To reject overlap events, we accept only events with no more than one reconstructed vertex within ± 60 cm from the center of the detector.

The method we use to search for a DD signal is based on the approximately flat dependence of the event rate on $\Delta\eta$ expected for DD events, as seen by setting $\alpha(t) = 0.1 + 0.25t$ in Eq. 3, compared to the exponential dependence expected for non-diffractive (ND) events where rapidity gaps are due to random multiplicity fluctuations. Thus, in a plot of event rate versus $\Delta\eta$, the DD signal will appear as the flattening at large $\Delta\eta$ of an exponentially falling distribution. For practical considerations, our analysis is based on *experimental* gaps defined as $\Delta\eta^0_{exp} \equiv \eta_{max} - \eta_{min}$, where (η_{min}) η_{max} is the η of the "particle" closest to $\eta = 0$ in the (anti)proton direction (see Fig. 1). A "particle" is a reconstructed track in the CTC, a calorimeter tower with energy above a given threshold, or a BBC hit. The (uncorrected) tower energy thresholds used, chosen to lie comfortably above noise level, are $E_T = 0.2$ GeV for the central and plug and $E = 1$ GeV for the forward calorimeters. At the calorimeter interfaces near $|\eta| \sim 0$, 1.1 and ~ 2.4, where the noise level is higher, $|\eta|$-dependent thresholds are used. The DD signal is extracted by fitting the measured $\Delta\eta^0_{exp}$ distribution with expectations based on a Monte Carlo (MC) simulation incorporating SD, DD and ND contributions. The same thresholds are used in the MC simulations after dividing the generated particle energy by an η-dependent energy calibration coefficient representing the ratio of true to measured (uncorrected) calorimeter energy [15]. For charged-particle tracks, the MC generation is followed by a detector simulation.

Figure 2 shows lego histograms of events versus η_{max} and $-\eta_{min}$ for data and for Monte Carlo generated ND, SD and DD events at $\sqrt{s} = 1800$ GeV. A uniform η-distribution was assumed for particles within a calorimeter tower. The observed structure in the distributions along $\eta_{max(min)}$ is caused by the variation of the tower energy threshold with $|\eta|$. The bins at $|\eta_{max(min)}| = 3.3$ contain all events within the BBC range of $3.2 < |\eta_{max(min)}| < 5.9$.

The diffractive Monte Carlo program is a modified version of that used in Ref. [16], incorporating the differential cross sections of Eqs. 1 and 3. Non-diffractive interactions are simulated using PYTHIA [17]. The data distribution in Fig. 2 has a larger fraction of events at large $|\eta_{max(min)}|$ than either the ND or the SD Monte Carlo generated distributions. From the previously measured SD cross section [11] and the MC determined fraction of SD events triggering both BBC arrays, the fraction of SD events in our 1800 [630] GeV data sample is estimated to be 2.7% [2.4%]. A combination of 97.3% ND and 2.7% SD generated events cannot account for the data at large $|\eta_{max(min)}|$ in Fig. 2. The simulated DD distribution is approximately flat in $|\eta_{max(min)}|$ and describes the data well when combined with the ND and SD distributions, as shown below.

Figure 3 presents the number of events as a function of $\Delta\eta^0_{exp}$ for the 1800 GeV data (points) and for a fit to the data using a mixture of MC generated DD and "non-DD" (ND plus SD) contributions (solid histogram). The dashed histogram shows the non-DD contribution. The agreement between data and MC indicates that, as in SD, the shape of the differential DD cross section is correctly described by Regge theory and factorization.

At $\sqrt{s} = 1800$ [630] GeV, the fraction of events with $\Delta\eta^0_{exp} > 3$ (gap fraction) is $(9.08 \pm 0.03)\%$ [$(11.43 \pm 0.03)\%$], in which the fraction of background non-DD events, estimated using the MC simulation, is $(23.6 \pm 0.6)\%$ [$(29.7 \pm 0.6)\%$]. After background subtraction, the DD gap fraction becomes $(6.94 \pm 0.06)\%$ [$(8.03 \pm 0.08)\%$]. The quoted errors are statistical. The amount of ND background in the region $\Delta\eta^0_{exp} > 3$ depends on the tower energy calibration coefficients and thereby on the calorimeter tower energy thresholds used in the MC. Increasing these thresholds has the effect of decreasing the multiplicity in the MC generated events, resulting in larger rapidity gaps and hence larger ND backgrounds in the region of $\Delta\eta^0_{exp}$. The systematic uncertainty in the background is estimated by raising (lowering) the tower thresholds in the MC by a factor of 1.25 and refitting the data. This change in thresholds increases (decreases) the background by a factor of 1.54 (0.52) [1.56 (0.56)].

The vertex cut employed to reject events due to multiple interactions also rejects single interaction events with extra (fake) vertices resulting from track reconstruction ambiguities. By comparing the fraction of events surviving the vertex cut with the fraction of single interaction events expected from the BBC cross section and the instantaneous luminosity, the vertex cut efficiency (fraction of single interaction events retained) is found to be 0.87 ± 0.02(syst) [0.90 ± 0.02(syst)]. In determining the DD gap fraction this efficiency is applied only to the total number of events, since the gap events have low central multiplicities and therefore are not likely to have fake vertices.

The measured DD gap fractions, which are based on our experimental gap definition, $\Delta\eta^0_{exp} \equiv \eta_{max} - \eta_{min}$, depend on the particle E_T thresholds used. The correction factors needed to transform the measured gap fractions to gap fractions corresponding to the gap definition on which Eq. 3 is based, namely $\Delta\eta^0 \equiv \ln \frac{ss_\circ}{M_1^2 M_2^2}$ ($\ln \frac{M_i^2}{\sqrt{ss_\circ}} < 0,\ i = 1,2$), were evaluated using the DD Monte Carlo simulation and found to be 0.81 [0.75] for $\sqrt{s} = 1800$ [630] GeV. Correcting the measured DD gap fractions by these factors and for the vertex cut efficiency, and normalizing the results to the previously measured cross sections of 51.2 ± 1.7 mb [39.9 ± 1.2 mb] for events triggering the BBC arrays, we obtain $2.51 \pm$

$0.01(\text{stat}) \pm 0.08(\text{norm}) \pm 0.58(\text{bg})$ mb [$2.16 \pm 0.01(\text{stat}) \pm 0.06(\text{norm}) \pm 0.65(\text{bg})$ mb] for the DD cross section in the region $\Delta\eta^0 > 3$.

The trigger acceptance, evaluated from the DD MC simulation, is $0.57 \pm 0.07(\text{syst})$ [$0.63 \pm 0.07)(\text{syst})$]. The uncertainty was estimated by considering variations in the simulation of small mass diffraction dissociation. The acceptance corrected DD cross sections for $\Delta\eta^0 > 3$ are $4.43 \pm 0.02(\text{stat}) \pm 1.18(\text{syst})$ mb [$3.42 \pm 0.01(\text{stat}) \pm 1.09(\text{syst})$ mb].

The corresponding cross sections predicted by Eq. 3, determined by the DD MC simulation, are 49.4 ± 11.1 (syst) mb [27.7 ± 5.5 (syst) mb], where the uncertainty is due to an assigned 10% systematic error in the triple-Pomeron coupling $g(0) = \kappa\beta(0)$ [9]. The ratio (discrepancy factor) of measured to predicted cross sections is $D_{DD} = 0.09 \pm 0.03$ [0.12 ± 0.03], where the errors include the statistical and all systematic uncertainties. Recalling that Eq. 3 correctly describes the shape of the $\Delta\eta^0$ distribution, the deviation of D from unity represents a breakdown of factorization affecting only the overall normalization. This result is similar to that observed in SD [9,12], where the corresponding discrepancy factors, calculated from the fit parameters in Ref. [9], are $D_{SD} = 0.11 \pm 0.01$ [0.17 ± 0.02].

Our data are compared with the UA5 results [3] in Fig. 4. The comparison is made for cross sections integrated over t and over all gaps of $\Delta\eta > 3$, corresponding to $\xi = e^{-\Delta\eta} = 0.05$ in SD. The extrapolation of our data from $\Delta\eta^0 > 3$ (gaps overlapping $\eta = 0$) to $\Delta\eta > 3$ (all gaps) was made using Eq. 3 and amounts to multiplying the $\Delta\eta^0 > 3$ cross sections by a factor of 1.43 (1.34) at $\sqrt{s} = 1800$ [630] GeV, yielding

$$\begin{gathered}\sigma_{DD}(\sqrt{s} = 1800\ [630]\ \text{GeV}, \Delta\eta > 3) = \\ 6.32 \pm 0.03(\text{stat}) \pm 1.7(\text{syst})\ \text{mb} \\ [4.58 \pm 0.02(\text{stat}) \pm 1.5(\text{syst})\ \text{mb}]\end{gathered} \tag{4}$$

The reported UA5 cross section values were obtained by extrapolating cross sections measured over limited large-gap regions to $\Delta\eta > 3$ using a Monte Carlo simulation in which the p and $\bar{p}$ dissociated independently with a $(1/M^2)e^{7t}$ distribution [18]. For a meaningful comparison, we corrected the reported UA5 values by backtracking to the measured limited

$\Delta\eta$ regions using a $(1/M^2)e^{7t}$ dependence and then extrapolating to $\Delta\eta > 3$ using Eq. 3. This correction increases the cross sections by a factor of 1.43 [1.19] at $\sqrt{s}$ = 200 [900] GeV. The solid curve in Fig. 4 was calculated using Eq. 3. The disagreement between this curve and the data represents the breakdown of factorization discussed above. The dashed curve represents the prediction of the renormalized gap probability model [12,10], in which the integral of the gap probability (first factor in Eq. 3 over all available phase space) is normalized to unity. The error bands around the curves are due to the 10% uncertainty in the triple-Pomeron coupling [9]. Within the quoted uncertainties, the data are in agreement with the renormalized gap model.

In conclusion, we have measured double diffraction differential cross sections in $\bar{p}p$ collisions at $\sqrt{s}$ =1800 and 630 GeV and compared our results with data at $\sqrt{s}$=200 and 900 GeV and with predictions based on Regge theory and factorization. We find a factorization breakdown similar in magnitude to that observed in single diffraction dissociation. The data are in agreement with the renormalized gap probability model [10].

We thank the Fermilab staff and the technical staffs of the participating institutions for their vital contributions. This work was supported by the U.S. Department of Energy and National Science Foundation; the Italian Istituto Nazionale di Fisica Nucleare; the Ministry of Education, Science, Sports and Culture of Japan; the Natural Sciences and Engineering Research Council of Canada; the National Science Council of the Republic of China; the Swiss National Science Foundation; the A. P. Sloan Foundation; the Bundesministerium fuer Bildung und Forschung, Germany; and the Korea Science and Engineering Foundation.

REFERENCES

[1] We use rapidity and pseudorapidity, η, interchangeably; $\eta \equiv -\ln(\tan\frac{\theta}{2})$, where θ is the polar angle of a particle with respect to the proton beam direction. The azimuthal angle is denoted by ϕ, and transverse energy is defined as $E_T = E\sin\theta$.

[2] P.D.B. Collins, *An Introduction to Regge Theory and High Energy Physics* (Cambridge University Press, Cambridge 1977).

[3] R. E. Ansorge *et al.*, Z. Phys. C **33**, 175 (1986).

[4] See A. Givernaud *et al.*, Nucl. Phys. B **152**, 189 (1979).

[5] C. Conta *et al.*, Nucl. Phys. B **175**, 97 (1980).

[6] C. Adloff *et al.*, Z. Phys. C **74**, 221 (1997).

[7] See K. Goulianos, Phys. Rep. **101**, 169 (1983).

[8] R.J.M. Covolan, J. Montanha and K. Goulianos, Phys. Lett. B **389**, 176 (1996).

[9] K. Goulianos and J. Montanha, Phys. Rev. D **59**, 114017 (1999).

[10] K. Goulianos, "Diffraction: Results and Conclusions", in *Proceedings of Lafex International School of High Energy Physics, Rio de Janeiro, Brazil, February 16-20 1998*, edited by Andrew Brandt, Hélio da Motta and Alberto Santoro; hep-ph/9806384.

[11] F. Abe *et al.*, Phys. Rev. D **50**, 5550 (1994).

[12] K. Goulianos, Phys. Lett. B **358**, 379 (1995).

[13] see, for example, E. Gotsman, E. Levin and U. Maor, Phys. Rev. D **60**, 094011, 1999.

[14] F. Abe *et al.*, Nucl. Instrum. Methods **A271**, 387 (1988).

[15] For details of the tower energy calibration procedure see: S. Bagdasarov, PhD thesis, Rockefeller University, 1997 (unpublished).

[16] F. Abe *et al.*, Phys. Rev. D **50**, 5535 (1994).

[17] T. Sjöstrand, Comp. Phys. Commun. **82**, 74 (1994).

[18] G. J. Alner *et al.*, Nucl. Phys. **B291**, 445 (1987).

FIGURES

FIG. 1. Schematic diagram and event topology of a double diffractive interaction, in which a Pomeron ($I\!\!P$) is exchanged in a $\bar{p}p$ collision at center-of-mass energy $\sqrt{s}$ producing diffractive masses M_1 and M_2 separated by a rapidity gap of width $\Delta\eta = \eta_{max} - \eta_{min}$. The shaded areas represent regions of particle production (mass and energy units are in GeV).

FIG. 2. The number of events as a function of η_{max} and $-\eta_{min}$, the η of the track or hit tower closest to $\eta = 0$ in the (anti)proton direction at $\sqrt{s} = 1800$ GeV: (a) data; (b, c, d) MC generated non-diffractive (ND), single- (SD) and double-diffractive (DD) events. The MC distributions are normalized by a fit to the data described in the text.

FIG. 3. The number of events as a function of $\Delta\eta^0_{exp} = \eta_{max} - \eta_{min}$ for data at $\sqrt{s} = 1800$ GeV (points), for double diffractive (DD) plus non-DD (MC) generated events (solid line), and for only non-DD MC events (dashed line). The non-DD events are a mixture of 96.7% non-diffractive and 3.3% single diffractive.

FIG. 4. The total double diffractive cross section for $p(\bar{p}) + p \rightarrow X_1 + X_2$ versus $\sqrt{s}$ compared with predictions from Regge theory based on the triple-Pomeron amplitude and factorization (solid curve) and from the renormalized gap probability model (dashed curve).

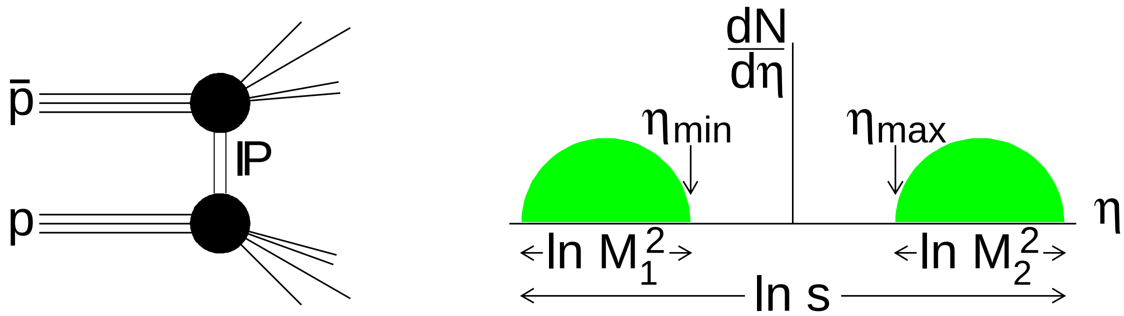

FIG. 1. Schematic diagram and event topology of a double diffractive interaction, in which a Pomeron ($I\!\!P$) is exchanged in a $\bar{p}p$ collision at center-of-mass energy $\sqrt{s}$ producing diffractive masses M_1 and M_2 separated by a rapidity gap of width $\Delta\eta = \eta_{max} - \eta_{min}$. The shaded areas represent regions of particle production (mass and energy units are in GeV).

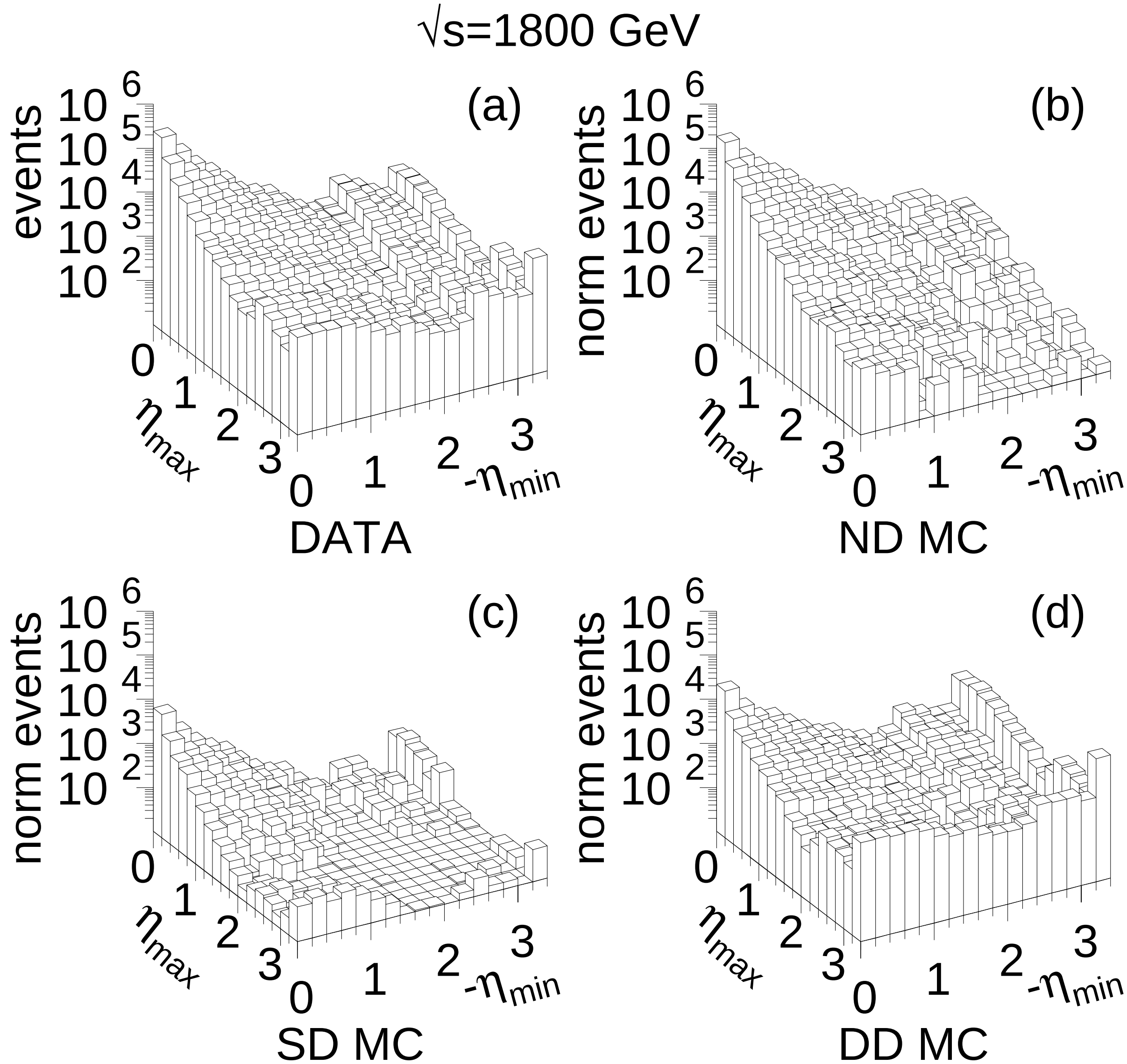

FIG. 2. The number of events as a function of η_{max} and $-\eta_{min}$, the η of the track or hit tower closest to $\eta = 0$ in the (anti)proton direction at $\sqrt{s} = 1800$ GeV: (a) data; (b, c, d) MC generated non-diffractive (ND), single- (SD) and double-diffractive (DD) events. The MC distributions are normalized by a fit to the data described in the text.

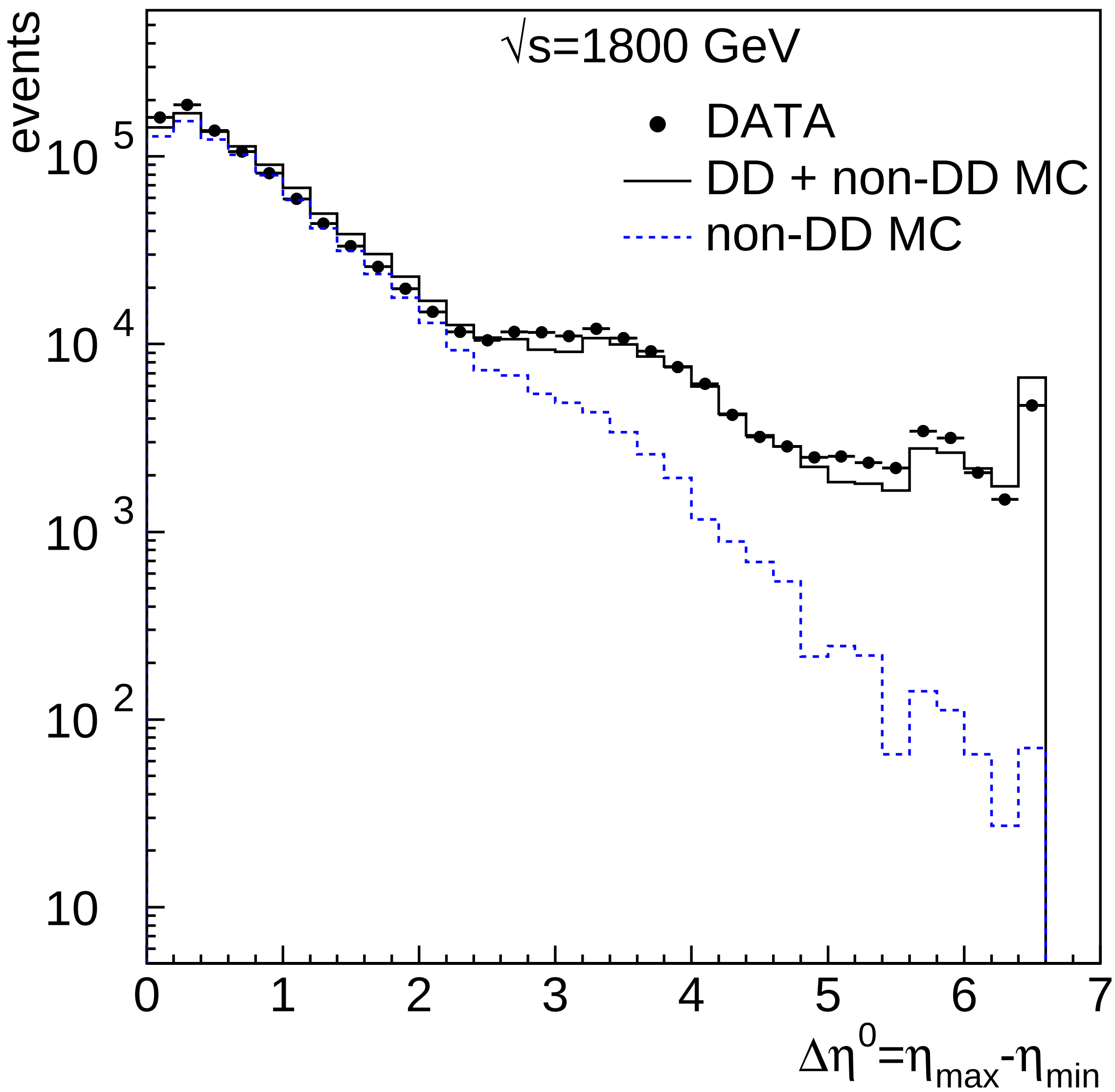

FIG. 3. The number of events as a function of $\Delta\eta^0_{exp} = \eta_{max} - \eta_{min}$ for data at $\sqrt{s} = 1800$ GeV (points), for double diffractive (DD) plus non-DD (MC) generated events (solid line), and for only non-DD MC events (dashed line). The non-DD events are a mixture of 97.3% non-diffractive and 2.7% single diffractive.

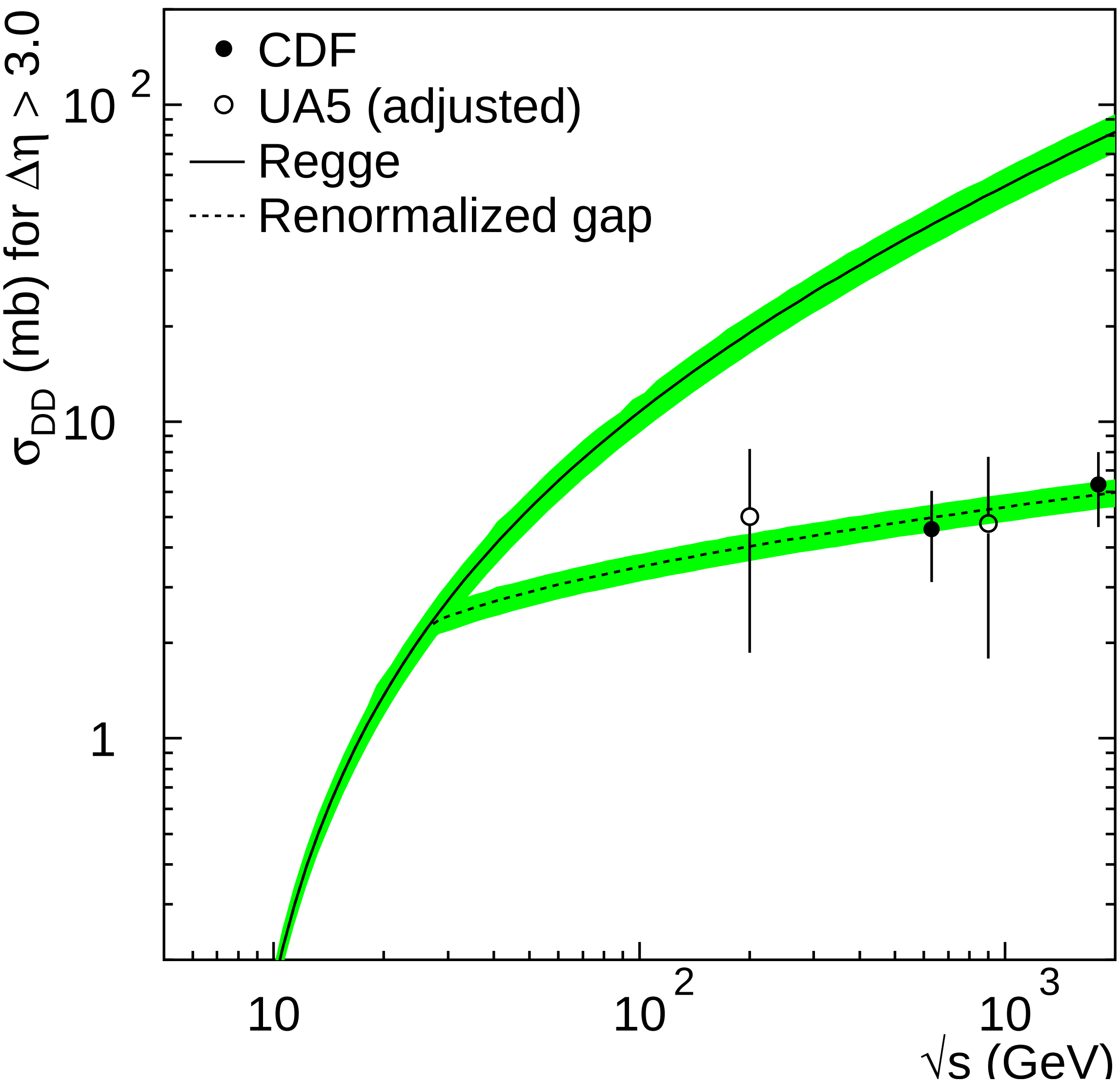

FIG. 4. The total double diffractive cross section for $p(\bar{p}) + p \to X_1 + X_2$ versus $\sqrt{s}$ compared with predictions from Regge theory based on the triple-Pomeron amplitude and factorization (solid curve) and from the renormalized gap probability model (dashed curve).